Cancer Management and Research

Elevate Series

Open Access Full Text Article

ORIGINAL RESEARCH

Establishment of Predictive Models for Second Hepatoma Recurrence

Miaotong Su[1,*], Weixiang Zhong[2,*], Zhen Chen[2], Guohong Zhang[1]

[1]Department of Pathology, Shantou University Medical College, Shantou, Guangdong, People's Republic of China; [2]Department of Pathology, the First Affiliated Hospital of Zhejiang University Medical College, Hangzhou, Zhejiang, People's Republic of China

*These authors contributed equally to this work

Correspondence: Guohong Zhang, Department of Pathology, Shantou University Medical College, 22 Xinling Road, Jinping District, Shantou, Guangdong, People's Republic of China, Email g_ghzhang@stu.edu.cn

Introduction: Given that hepatoma frequently recurs after initial resection, it is often managed by liver transplantation. The persistently high recurrence rate even after transplantation underscores the need for better prognostic tools. Enhancing prediction accuracy before a second intervention is key to optimizing postoperative care and improving outcomes. We assessed which clinicopathological factor or molecular biomarkers could be optimally constructing prediction models to assist the treatment after resections, and prepare to second surgery.

Methods and Material: To develop predictive models, we first evaluated CD46 and CD47 expression by immunohistochemistry using tissue microarrays from 196 patients who underwent resection for recurrent hepatoma. We then employed an artificial neural network and a classification and regression tree to optimize models that combined these biomarkers with pertinent clinical factors.

Results: Survival analysis revealed that CD47 expression was significantly associated with both disease-free survival (DFS) and disease-specific survival (DSS) in patients experiencing a second recurrence. Significant differences in pathologic type, vein tumor thrombosis, Milan criteria, and CD47 expression were observed between patients with and without second recurrence. Likewise, these same factors—pathologic type, satellite lesions, Milan criteria, and CD47—also distinguished patients who died from a second recurrence from those with other outcomes ($P < 0.05$). By integrating these predictors, we developed classification models that achieved an accuracy of 85.0% for predicting second postoperative recurrence and 80.0% for predicting postoperative disease-specific prognosis.

Conclusion: We present multi-factor models that predict second recurrence and prognosis in recurrent HCC. This prognostic tool can inform personalized clinical management after resection and improve decision-making prior to transplantation.

Keywords: hepatoma, liver tissue-on-chip, immunohistochemistry, prognosis

Introduction

Hepatoma remains one of the leading causes of cancer-related deaths.[1] The high rate of tumor recurrence after hepatectomy, which can be as high as 50%–70% at 5 years after surgery.[2] For those with recurrent hepatoma, liver transplantation is acceptable However, the 5-year tumor recurrence rate after transplantation also remains high, and the majority of patients die from early-recurrence within 2 years.[3] Enhancing the prediction accuracy for prognosis before second operations should be effective to facilitate postoperative management for recurrent patients and reduce the risk of recurrence after second operations.

Common surveillance protocols for detecting tumor recurrence after the surgery has limitations.[4] Little commonly used tumor biomarkers are immune-related biomarkers. In recent years, more studies have found that the immune microenvironment has a significant influence on the development of hepatoma.[5] Therefore, we reviewed the literatures and chose immune-related biomarkers which should be expressed on tumor or immune cells. Two candidate markers were identified, CD46 and CD47, that met the above criteria.

Activation of the complement system leads to a series of cellular responses, ranging from cellular apoptosis to opsonization.[6] Overactivation of the complement system results in auto-immune damage to the organism. So for injury

https://doi.org/10.2147/CMAR.S566522
Received: 9 September 2025
Accepted: 27 January 2026
Published: 24 March 2026

prevention, several membrane complement regulatory proteins are expressed on host cells to inhibit the overactive complement system, including CD46,[7] which has been reported to be associated with cancer-associated resistance mechanisms[8] and shows an elevated expression level in several different malignancies, including hepatoma.[9,10] Several studies have found that CD46 plays a significant role in hepatoma carcinogenesis[11] and confers poor prognosis.[10] CD47 can prevent phagocytosis by macrophages, is expressed on most plasma membranes of immune, and parenchymal cells, indicating that cells with lower expression of CD47 will be engulfed by macrophages. In the case of tumor cells, overexpressing CD47 will prevent their phagocytic uptake by macrophages.[12–15] Chen et al found that increasing CD47 expression in hepatoma tissues was positively correlated with macrophage density and poor prognosis in hepatoma patients.[16] Also, CD47 expression was found to be higher in early-recurrent hepatoma patients than in primary hepatoma patients in single-cell sequencing.[17] CD47 has become an emerging therapeutic target for anti-tumor treatment.

To sum up, they are shown to be important in prognosis of hepatoma patients in some way. We decided chose them as biomarkers to constructed the multi-factor prediction models. Classification and regression tree (CART) is commonly used in clinical therapy, which appears to be intuitive and straightforward to assign patients into subgroups by using a dendrogram.[18] In this study, we analyzed investigated the expression of CD46 and CD47 in human hepatoma by immunohistochemical staining, and investigated the correlation between the expression and clinicopathological characteristics. According to the level of expression of them, we performed survival analysis to determine their survival curves. Then univariate and multivariate logistic regression analyses were used to identify clinicopathological factors and markers as predictors. Finally, an artificial neural network (ANN) and classification and regression tree (CART) models were carried out to construct a model for the prediction of prognosis and survival after surgery. The receiver operating characteristic (ROC) curve was constructed and K-fold cross-validation was employed to describe and examine the accuracy of the model.

Materials and Methods

Patients

One hundred ninety-six Chinese patients, between 2015 and 2019, who had already received liver resection at the First Affiliated Hospital, College of Medicine, Zhejiang University were enrolled in this study, as well as 53 patients with hepatic hemangioma who served as non-carcinoma controls. All patients had recurrence after resection and would undergo liver transplantation as well. Doctors took samples of their tumors before second surgeries. Disease-free survival (DFS) was defined as the interval from the date of second operation to recurrence. If we did not observe recurrence, then DFS was defined as the last follow-up time. The binary outcome was “Yes” or “No.” A positive event was defined as radiologically confirmed intrahepatic or extrahepatic recurrence following the first recurrence. Disease-specific survival (DSS) was defined as the time from the date of surgery to death due to second recurrence, or the last follow-up. It is worth noting that the outcomes with a final DSS definition of death must be death from recurrence of hepatoma. The binary outcome was “Yes” or “No.” A positive event was defined as death conclusively attributed to the progression of recurrent hepatoma. Deaths from other causes were censored. Pathologists examined patient H&E-stained slides and all reports and records to identify and collect the clinicopathological characteristics. Control group samples were confirmed to para-hepatic hemangioma area tissues.

Patients provided written informed consent for use of all samples in this study, and the protocol was approved by the Clinical Research Ethic Committee of the First Affiliated Hospital, Zhejiang University School of medicine. Our study complies with the Declaration of Helsinki.

Furthermore, we incorporated the level 3 hepatoma-associated mRNA expression matrix and clinical data of 374 hepatoma patients and 50 normal controls, from the GDC TCGA-LIHC (https://www.cancer.gov/ccg/research/genome-sequencing/tcga) cohort.

Tissue Microarray Construction

Paraffin tissue blocks were used to construct the tissue microarray (TMA), by a manual tissue microarrayer (TMA Grand Master, 3dHISTECH, Hungary), and pathologists took cores for different tissues Those regions were selected for H&E staining (Fig. S1A). Then those regions are marked on each donor block, and drilling tissue cylinders (2 mm diameter) shifted them to recipient blocks.

Data Collection and Validation

To verify that the biomarker selection was feasible, we first downloaded the GDC TCGA-LIHC cohort from USCS XENA, including the level 3 hepatoma-associated mRNA expression matrix and clinical data from 374 patients and 50 normal control samples. Then, we compare the CD46 and CD47 levels versus survival in patients through GraphPad Prism software.

Immunohistochemistry and Image Analysis

TMA sections were baked at 62°C for 3 hours, dewaxed in xylene, and rehydrated through a gradient ethanol series. After washes in distilled water, we placed TMA sections in 0.3% hydrogen peroxide at room temperature. Antigen retrieval was performed by heating the sections in 10 mM citrate buffer for 5 min. Then TMA sections were incubated with anti-CD46 antibody (1:200, Abcam, ab108307) or anti-CD47 antibody (1:200, Abcam, ab218810) overnight at 4°C. Tissues were incubated with second antibody (MaxVision-HRP mouse/rabbit, Kit-5020, MXB Biotechnologies) for 30 min at 37°C, and developed with 3,3′-diaminobenzidine (DAB, DAB-0031, MXB Biotechnologies) for 30 seconds, followed by counterstaining with hematoxylin and sealing with coverslips.

We assessed the level of CD46 and CD47 expression by using a CaseViewer image analysis system (3DHISTECH). For quantitation, QuantCenter (3DHISTECH) image analysis software was used to analyze the IHC staining intensity of each image by identifying the cell membrane. Staining intensity was classified in one of the following categories: no staining (0), weak (1), moderate (2), and strong (3). Then to the H-score was determined by the following: H-score= [(1* weak staining area%) + (2*moderate staining area%) + (3*strong staining area%). H-scores ranged from 0–300 and were used to judge the cell membrane staining (Figure S1B). For each TMA section, five random 40× microscopic fields were selected from each TMA section for scoring. In cases with limited tissue, a minimum of three fields was ensured. The average score from these fields was taken as the final result. We also verified that no tissue detachment occurred on any of the sections. We performed receiver operating characteristic (ROC) curves to determine the cut-off points for the level of CD46 and CD47 expression.

Statistical Analysis

Continuous variables with normal distribution were compared using the two-tailed Student's *t*-test and are presented as mean ± SD. Categorical variables were compared using the chi-square test, while correlations were assessed with the Pearson coefficient.

Survival analyses for overall survival (OS), disease-free survival (DFS) and disease-specific survival (DSS) were performed using the Kaplan–Meier method, with comparisons between groups made by the Log rank test. Univariate and multivariate logistic regression analyses (significance level $P < 0.05$) were conducted to evaluate the predictive ability of clinicopathological factors and biomarkers. They were employed to identify factors independently associated with our binary endpoints (second recurrence and disease-specific death), while controlling for potential confounders.

Receiver operating characteristic (ROC) curves and the area under the curve (AUC) were used to evaluate the specificity and sensitivity of each predictor. An artificial neural network (ANN) was optimized and assessed using training and testing sets to determine prediction accuracy. For recurrence and prognosis prediction, a classification and regression tree (CART) model was employed to identify clinicopathological characteristics and biomarkers that optimize diagnostic accuracy for postoperative second recurrence and disease-specific outcomes in recurrent hepatoma patients. To evaluate model performance, mitigate dataset partition bias, and assess overfitting, k-fold cross-validation was applied (k = 10, repeated 200 times) using the standard error rule. The purpose of ANN and CART models was to develop and

optimize integrated classification models for predicting the two clinical endpoints and to compare the performance of these different algorithms.

ROC analysis, CART modeling, and cross-validation were performed using R packages (pROC, rpart, caret). All other statistical analyses were conducted in SPSS version 23.0. A two-tailed p-value < 0.05 was considered statistically significant.

Results

Preliminary Validation

From the GDC TCGA-LIHC cohort, we extracted the level 3 hepatoma-associated mRNA expression matrix and clinical data of 374 hepatoma patients and 50 normal controls. PCA (principal component analysis) was used to differentiate all the samples from the TCGA cohort (Figure 1A). The correlation (Figure 1B and C) and differentiation (Figure 1D and E) between the expression of CD46 and CD47 in hepatoma patients and normal controls were analyzed. Pearson correlation and two-tailed Student's *t*-test showed CD46 and CD47 were positively correlated in both tumor tissues and normal controls, and patients had higher expression of CD46 and CD47 when compared with normal controls, indicating that both biomarkers are associated with tumorigenesis. Analysis of OS further showed a correlation between low expression levels of CD46 and CD47 with the poor clinical prognosis (Figure 1F and G), and the performance of CD47 was more significant.

Patient Characteristics

The clinicopathological factors of all patients are summarized in Table 1.

The mean follow-up time was 530.16 days (range 1–1597), and the median follow-up period was 447.5 days (interquartile range (IQR) 240–707.5). As for treatment, all patients received liver resection and would receive liver transplantation, and it is unknown whether they received other therapies.

For all cases, 64/196 (32.65%) patients developed second recurrence during follow-up period, and 36.22% of the patients (71/196) died, wherein 18.37% (36/196) died of second recurrence of the original carcinoma during the period. The 1-, 2-, and 3-year OS rates were 74.9%, 55.2%, and 53.6%, the 1-, 2-, and 3-year DFS rates were 69.0%, 58.8%, and 53.9%, and the 1-, 2-, and 3-year DSS rates were 90.0%, 80.1%, and 68.7%, respectively.

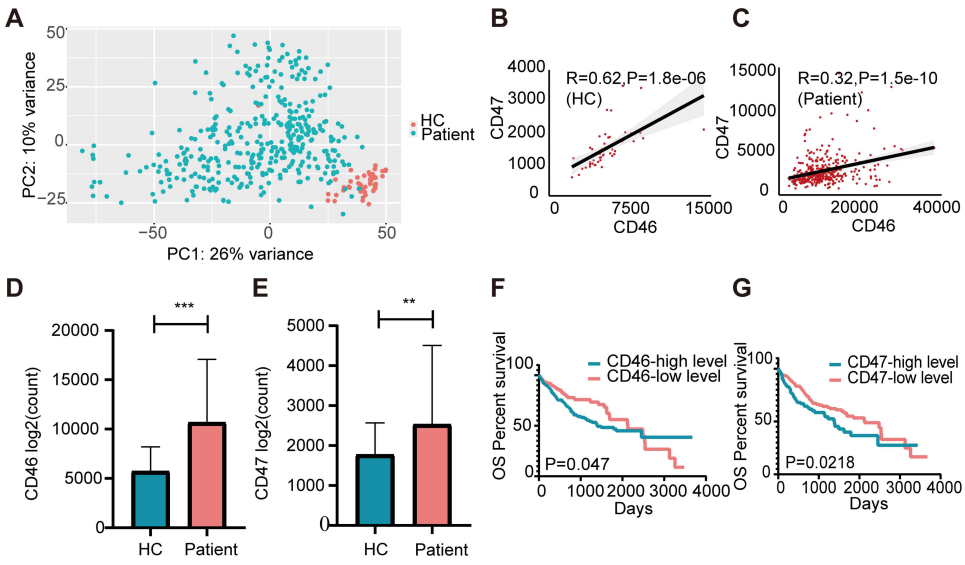

Figure 1 Expression of CD46 and CD47 in GDC TCGA-LIHC. (**A**) Sample clustering by PCA in the GDC TCGA-LIHC dataset of 374 tumor and 50 healthy tissues. (**B**) The correlations between CD46 and CD47 in the healthy control cohort. (**C**) The correlations between CD46 and CD47 in the tumor cohort. (**D**) The expression of CD46 in liver cancer tissue and healthy tissue. ***$P<0.001$. (**E**) The expression of CD47 in liver cancer tissue and healthy tissue. **$P<0.01$. (**F**) Log rank test and KM survival curve analysis according to the expression of CD46. (**G**) Log rank test and KM survival curve analysis according to the expression of CD47.

https://doi.org/10.2147/CMAR.S566522

Table 1 Clinicopathological Factors of Patients with Hepatoma

Variables	Number (n=196)	Percent
Age		
≤53	107	54.59
>53	89	45.41
Gender		
Male	176	89.8
Female	20	10.2
Pathologic Type		
HCC	150	76.53
ICC	34	17.35
HCC-ICC	12	6.12
Tumor number		
Single	86	43.88
Multiple	110	56.12
Maximum tumor diameter (cm)		
≤5	134	68.37
>5	62	31.63
Milan Criteria		
Substandard	122	62.24
Standard	74	37.76
Tumor differentiation		
I	5	2.55
II	71	36.23
III	119	60.71
IV	1	0.51
Satellite lesions		
No	108	55.1
Yes	88	44.9
Vein tumor thrombosis		
No	104	53.06
Yes	92	46.94
MVI		
No	74	37.76
Low risk	64	32.65
High risk	58	29.59
Capsular invasion		
No	147	75
Yes	49	25
Bile duct invasion		
No	167	85.2
Yes	29	14.8
Nerve invasion		
No	190	96.94
Yes	6	3.06
TNM stage		
I	114	58.16
II	73	37.25
III	4	2.04
IV	5	2.55

(*Continued*)

https://doi.org/10.2147/CMAR.S566522

Table 1 (Continued).

Variables	Number (n=196)	Percent
MELD		
<12	94	47.96
≥12	102	52.04
AFP (ng/mL)		
≤25.0	95	48.47
>25.0	101	51.53

Abbreviations: HCC, hepatocellular carcinoma; ICC, intrahepatic cholangiocarcinoma; MVI, microvascular invasion; MELD, model for end-stage liver disease; AFP, alpha-fetoprotein.

Expression and Prognostic Value of CD46 and CD47 in Hepatoma

Immunohistochemistry (IHC) staining (Figure 2A and B) showed that tumor cells had a relatively high level of CD46 and CD47 expression compared to hepatocytes of the non-tumor region, and para-tumor tissue (Figure 2C and D). We also found that despite tumor cells having the highest level of CD46 and CD47 expression, normal tissues showed high level as well. Cells in the para-cancer and boundary (para-cancer) regions showed the lowest level of CD46 and CD47 expression. Comparing the CD46 and CD47 expression scores of tumor and non-tumor tissues, division of all patients into two groups (high-level and low-level expression) based on the cut-off points (CD46 H-score=116.75, CD47 H-score=106.1, respectively;).

Subsequent survival analysis showed that there was no prognostic significance between CD46 expression and any type of survival (Figure 2E, G, I), but patients with high-level CD47 expression were associated with longer disease free survival (median DFS, 382 days; 3-year DFS, 82.2%) and disease-specific survival (median DSS, 419 days; 3-year DSS, 88.5%) than those in patients with low-level CD47 expression (median DFS, 467 days; 3-year DFS, 60.3%; median DSS, 276 days; 3-year DSS, 50.8%), which was verified by Kaplan–Meier survival analysis (Figure 2F, H, J). Therefore, the DFS and DSS of recurrent hepatoma patients were negatively correlated with the CD47 expression in tumor cells, which appears to verify the data of TCGA-LIHC dataset, and correlation analysis (Figure 2K and L) showed the week correlation of CD47 in tumor tissues and normal controls.

Chi-square analysis showed that CD46 was related to vein tumor thrombosis, TNM stage and MELD score (Table 2), whereas the expression of CD47 on tumor cells was significantly associated with maximum tumor diameter, vein tumor thrombosis, capsular invasion, MVI and TNM stage of patients with hepatoma (Table 3). These results imply that expression of CD46 and CD47 are mainly associated with adverse clinicopathological features of hepatoma.

Diagnostic Accuracy of Clinicopathological Factors and CD47 for Second Recurrence and Prognosis of Hepatoma

Initially, each of the 16 clinicopathological factors and 2 markers was evaluated individually for its ability to predict patient outcomes using univariate logistic regression analysis. We entered them that achieved significance at $P < 0.1$, from the univariate analysis, into the multivariate logistic regression model. The results of both the univariate and multivariate analysis with the logistic regression model are listed in Tables 4 and 5.

Using univariate and multiple logistic regression analyses, there was a statistically significant difference for pathologic type, vein tumor thrombosis, Milan criteria and CD47 in predicting second recurrent patients vs. non second recurring patients (Table 4).

Similarly, pathologic type, Milan criteria, satellite lesions and CD47 had the most significant statistical differences in predicting patients who died of second recurrence vs. patients with other outcomes (Table 5). It follows that pathologic types had the most significant statistical difference in both regression models.

Based on those independent variables, two ROC curves of each independent predictor were generated (Tables 6 and 7, and Figure 3A and B), and verified the limited capacity for prediction of single clinical features. The results showed that

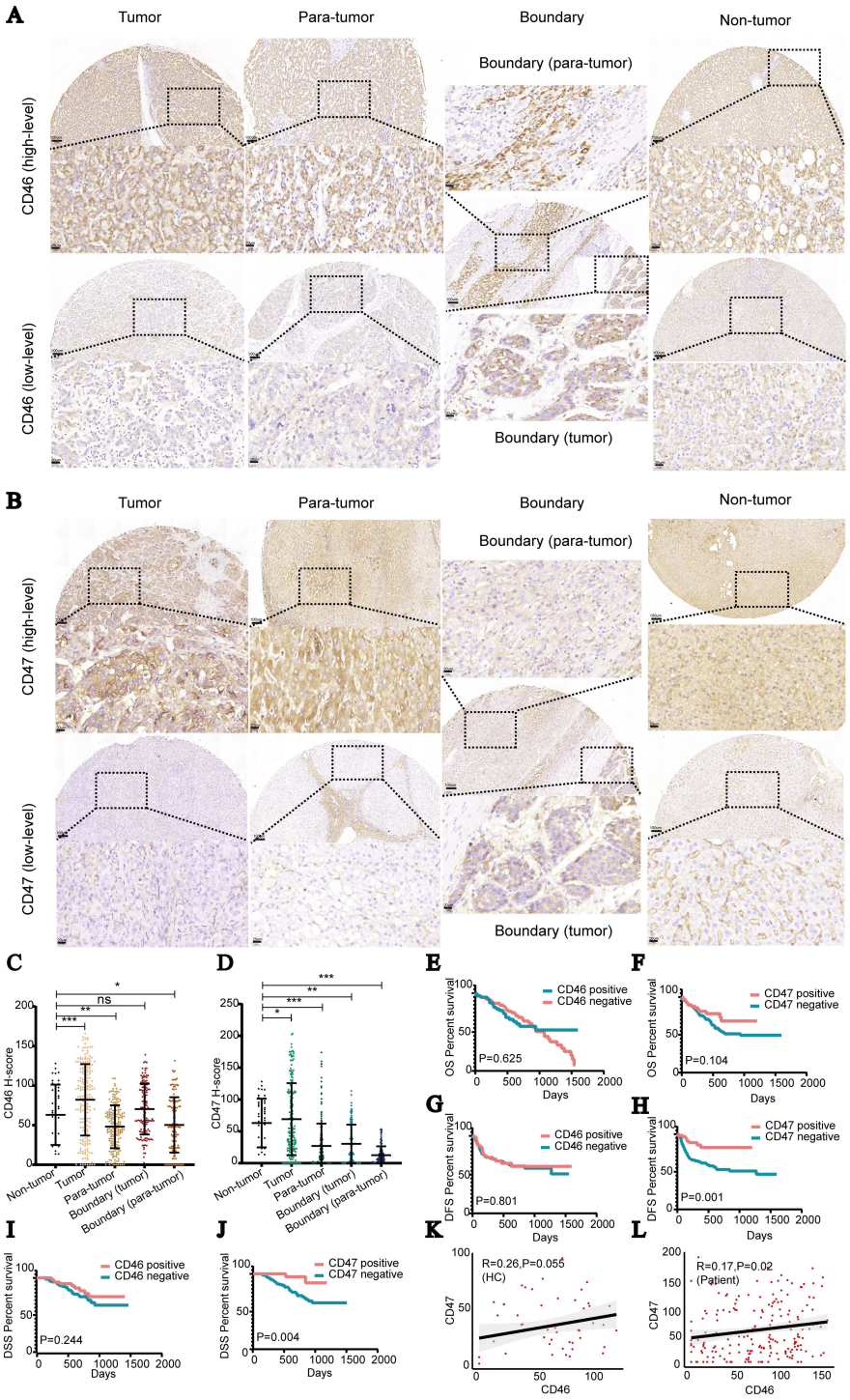

Figure 2 Expression of CD46 and CD47 in different tumor regions and clinical significance. (**A**) Representative microphotographs of CD46 immunostaining in tumor tissue, para-tumor tissue, boundary tissue, and normal control tissue. An H-score = 116.75 was used as the cut-off point to divide patients with low-level and high-level expression. Scale bar indicates 100 μm and 20 μm. (**B**) Representative microphotographs of CD47 immunostaining in tumor tissue, para-tumor tissue, boundary tissue, and normal control tissue. An H-score = 106.1 was used as the cut-off point to divide patients with low-level and high-level expression. Scale bar indicates 100 μm and 20 μm. (**C**) Discrepancy between CD46 expression level and different regions. Data shown as mean ± SD. ****P*<0.001, ***P*<0.01, **P*<0.05, ns *P* > 0.05. (**D**) Discrepancy between CD47 expression level and different regions. Data shown as mean ± SD. ****P*<0.001, ***P*<0.01, **P*<0.05. (**E**) Kaplan–Meier plots of overall survival (OS) rates based CD46 expression by section. The p-value was calculated by the Log rank test. (**F**) Kaplan–Meier plots of overall survival (OS) rates based CD47 expression by section. The p-value was calculated by the Log rank test. (**G**) Kaplan–Meier plots of disease-free survival (DFS) rates based on CD46 expression by section. P-value was calculated by the Log rank test. (**H**) Kaplan–Meier plots of disease-free survival (DFS) rates based on CD47 expression by section. P-value was calculated by the Log rank test. (**I**) Kaplan–Meier plots of disease-specific survival (DSS) rates based on CD46 expression by section. P-value was calculated by the Log rank test. (**J**) Kaplan–Meier plots of disease-specific survival (DSS) rates based on CD47 expression by section. P-value was calculated by the Log rank test. (**K**) Correlations between CD46 and CD47 in healthy tissue. The Pearson coefficient was applied for the correlation test. (**L**) Correlations between CD46 and CD47 in tumor tissue. The Pearson coefficient was applied for the correlation test.

https://doi.org/10.2147/CMAR.S566522

Table 2 Correlation Between CD46 Expression and Clinicopathological Factors in Hepatoma

Variables	CD46 Expression		*P*-value
	High Level (n(%)) n=57	Low Level (n(%)) n=139	
Age			0.504
≤53	29(27.10)	78(72.90)	
>53	28(31.46)	61(68.54)	
Gender			0.196*
Female	3(15.00)	17(85.00)	
Male	54(30.68)	122(69.32)	
Pathologic Type			0.279
HCC	46(31.08)	102(68.92)	
ICC/Others	11(22.92)	37(77.08)	
Tumor number			0.206
Single	28(25.45)	82(74.55)	
Multiple	29(33.72)	57(66.28)	
Maximum tumor diameter (cm)			0.492
≤5	41(30.60)	93(69.40)	
>5	16(25.81)	46(74.19)	
Milan criteria			0.146
Standard	26(35.14)	48(64.86)	
Substandard	31(25.41)	91(74.59)	
Tumor differentiation			0.114
I–II	27(35.53)	49(64.47)	
III–IV	30(25.00)	90(75.00)	
Satellite lesions			0.146
No	36(33.33)	72(66.67)	
Yes	21(23.86)	67(76.14)	
Vein tumor thrombosis			0.015
No	38(36.54)	66(63.46)	
Yes	19(20.65)	73(79.35)	
MVI			0.866
No	21(28.38)	53(71.62)	
Low-risk/high-risk	36(29.51)	86(70.49)	
Capsular invasion			0.057
No	48(33.33)	99(66.67)	
Yes	9(18.37)	40(81.63)	
Bile duct invasion			0.848
No	49(29.34)	118(70.66)	
Yes	8(27.59)	21(72.41)	
Nerve invasion			0.184*
No	57(30.00)	133(70.00)	
Yes	0(0)	6(100)	
TNM stage			0.007
I	38(33.33)	76(66.67)	
II–IV	19(23.17)	63(76.83)	
MELD score			0.046
<12	21(22.34)	73(77.66)	
≥12	36(35.29)	66(64.71)	
AFP (ng/mL)			0.254
≤25.0	24(25.26)	71(74.74)	
>25.0	33(32.67)	68(67.33)	

Note: *Fisher's precision probability test.

Table 3 Correlation Between CD47 Expression and Clinicopathological Factors in Hepatoma

Variables	CD47 Expression		*P*-value
	High Level (n(%)) n=57	Low Level (n(%)) n=139	
Age			0.193
≤53	27(25.23)	80(74.77)	
>53	30(33.71)	59(66.29)	
Gender			0.671
Female	5(25.00)	15(75.00)	
Male	52(29.55)	124(70.45)	
Pathologic Type			0.104
HCC	48(32.00)	102(68.00)	
ICC/others	9(19.57)	37(80.43)	
Tumor number			0.114
Single	30(34.88)	56(65.12)	
Multiple	27(24.55)	83(75.45)	
Maximum tumor diameter (cm)			0.041
≤5	45(33.58)	89(66.42)	
>5	12(19.35)	50(80.65)	
Milan Criteria			0.146
Standard	26(35.14)	48(64.86)	
Substandard	31(25.41)	91(74.59)	
Tumor differentiation			0.208
I–II	26(34.21)	50(65.79)	
III–IV	31(25.83)	89(74.17)	
Satellite lesions			0.146
No	36(33.33)	72(66.67)	
Yes	21(23.86)	67(76.14)	
Vein tumor thrombosis			0.015
No	38(37.50)	66(62.50)	
Yes	19(20.65)	73(79.35)	
MVI			0.006
No	30(40.54)	44(59.46)	
Low-risk/high-risk	27(22.13)	95(77.87)	
Capsular invasion			0.023
No	49(33.33)	98(66.67)	
Yes	8(16.33)	41(83.67)	
Bile duct invasion			0.074*
No	53(31.74)	114(68.26)	
Yes	4(13.79)	25(86.21)	
Nerve invasion			0.674*
No	56(29.47)	134(70.53)	
Yes	1(16.67)	5(83.33)	
TNM stage			0.012
I	41(35.96)	73(64.04)	
II–IV	16(19.51)	66(80.49)	
MELD			0.249
<12	31(32.98)	63(67.02)	
≥12	26(25.49)	76(74.51)	
AFP (ng/mL)			0.091
≤25.0	33(34.74)	62(65.26)	
>25.0	24(23.76)	77(76.24)	

Note: *Fisher's precision probability test.

Table 4 Discrimination of Prognostic Outcomes (Non-second Recurrence and second Recurrence) via Univariate and Multivariate Logistic Regression Analysis

Variables	Univariate	Multivariate		
	P-value	OR	95% CI	*P*-value
Gender (female/male)	0.444			
Age (≤53/>53)	0.916			
Pathologic Type (ICC+others/HCC)	<0.001	6.930	2.835–16.937	<0.001
Tumor number (multiple/single)	0.063	1.808	0.866–3.775	0.069
Maximum tumor diameter (>5cm/≤5cm)	0.005	1.402	0.799–2.458	0.449
Milan Criteria (substandard/standard)	<0.001	3.867	1.415–10.568	0.008
Tumor differentiation (I–II/III/IV)	0.035	1.214	0.474–3.111	0.664
Satellite lesions (yes/no)	<0.001	1.451	0.429–4.905	0.302
Vein tumor thrombosis (yes/no)	<0.001	4.402	1.863–10.401	0.001
MVI (low risk-high risk/no)	<0.001	3.201	1.104–9.276	0.099
Capsular invasion (yes/no)	<0.001	1.156	0.316–2.887	0.761
Bile duct invasion (yes/no)	<0.001	2.185	1.242–3.842	0.061
Nerve invasion (yes/no)	0.096	1.119	0.353–1.449	0.514
TNM stage (I/II–IV)	<0.001	1.551	0.494–4.866	0.755
AFP (>25ng/mL/≤25ng/mL)	0.003	1.730	0.723–4.138	0.142
MELD (<12/≥12)	0.691			
CD46 (high-level/low-level)	0.897			
CD47 (high-level/low-level)	0.001	0.262	0.097–0.707	0.008

Table 5 Discrimination of Prognostic Outcomes (Other Outcomes and Died of second Recurrence) via Univariate and Multivariate Logistic Regression Analysis

Variables	Univariate	Multivariate		
	P-value	OR	95% CI	*P*-value
Gender (female/male)	0.682			
Age (≤53/>53)	0.815			
Pathologic Type (ICC+others /HCC)	<0.001	8.567	3.307–22.193	<0.001
Tumor number (multiple/single)	0.005	1.807	0.537–6.083	0.339
Maximum tumor diameter (>5cm/≤5cm)	0.808			
Milan Criteria (substandard/standard)	<0.001	5.178	1.256–21.354	0.023
Tumor differentiation (I–II/III/IV)	0.548			
Satellite lesions (yes/no)	<0.001	4.987	1.620–15.354	0.005
Vein tumor thrombosis (yes/no)	<0.001	1.723	0.117–4.470	0.727
MVI (low risk-high risk/no)	<0.001	1.764	0.140–4.167	0.756
Capsular invasion (yes/no)	<0.001	1.389	0.484–3.986	0.542
Bile duct invasion (yes/no)	<0.001	2.384	0.827–6.875	0.108
Nerve invasion (yes/no)	0.349			
TNM stage (I/II–IV)	<0.001	2.693	0.771–9.407	0.120
AFP (>25ng/mL/≤25ng/mL)	0.205			
MELD (<12/≥12)	0.841			
CD46 (high-level/low-level)	0.551			
CD47 (high-level/low-level)	0.003	0.097	0.019–0.492	0.005

Table 6 Diagnostic Accuracy for DFS via Sensitivity and Specificity of Each Variable

Variables	Sensitivity, %	Specificity, %	AUC
Pathologic type	0.531	0.909	0.720
Vein tumor thrombosis	0.828	0.705	0.766
Milan criteria	0.875	0.500	0.688
CD47	–	–	0.377

Table 7 Diagnostic Accuracy for DSS via Sensitivity and Specificity of Each Variable

Variables	Sensitivity, %	Specificity, %	AUC
Pathologic type	0.667	0.863	0.765
Satellite lesions	0.644	0.861	0.752
Milan criteria	0.444	0.917	0.68
CD47	–	–	0.356

vein tumor thrombosis and pathologic type should be the factors with the best predictive ability. However, the predictive capability of individual factors was still not high enough. Thus, we chose to construct a model with multiple factors to enhance the distinguishing capability.

Construction of an Artificial Neural Network for Independent Factors

We used ANN-based approaches with 3-layer networks and the relative weights of neurons to predict the prognosis of recurrent hepatoma patients before the second surgery. The model, which predicts second-recurrent patients vs. no-second-recurrent patients, included 4 inputs (pathologic type, vein tumor thrombosis, Milan criteria, and CD47), 1 bias neuron in the input layer, 2 hidden neurons, 1 bias neuron in the hidden layer, and 2 output neurons (Figure 3C). The activation functions of the logistic sigmoid and hyperbolic tangent were used in each neuron of the hidden layer and output layer, respectively. The ANN correctly classified 78.1% of patients in the training and 80.0% of patients in the testing datasets (Figure 3D). The AUC for ANN on prediction was 87.6% for both second-recurrent patients and no-second-recurrent patients (Figure 3E).

Similarly, the model, which predict patients who died of second recurrence vs. patients who had other outcomes, also included 4 inputs (pathologic type, satellite lesions, Milan criteria, and CD47), 1 bias neuron in the input layer, 2 hidden neurons, 1 bias neuron in the hidden layer, and 2 output neurons (Figure 3F). The ANN correctly classified 79.0% of patients in the training and 87.9% of patients in the testing datasets (Figure 3G). The AUC for ANN on prediction were 89.2% for both patients who died of second recurrence and patients with other outcomes (Figure 3H). The overall performance of the ANN was consistent with the results obtained by ROC curve analysis.

Construction of Classification and Regression Tree for Independent Factors

We performed classification and regression tree (CART) analysis to distinguish recurrent from non-recurrent patients using the aforementioned factors. The model was trained on 137 randomly selected hepatoma cases and validated on an independent set of 59 cases (Figure 4A). Variable importance ranking indicated that pathologic type was the primary classifier, while CD47 contributed less significantly (Figure 4B). According to the confusion matrix (Figure 4C), the model performed comparably in classifying non-second-recurrent (84.21%) and second-recurrent patients (85.71%). The CART model (Figure 4D) achieved a sensitivity of 85.7%, specificity of 84.2%, and an AUC of 85.0%. The mean accuracy estimated via K-fold cross-validation (K=10, repetitions=200) was 80.0%.

A second CART model was developed to predict patients who died from second recurrence versus those with other outcomes (Figure 4E). Pathologic type remained the primary determinant, with CD47 emerging as the second most

https://doi.org/10.2147/CMAR.S566522

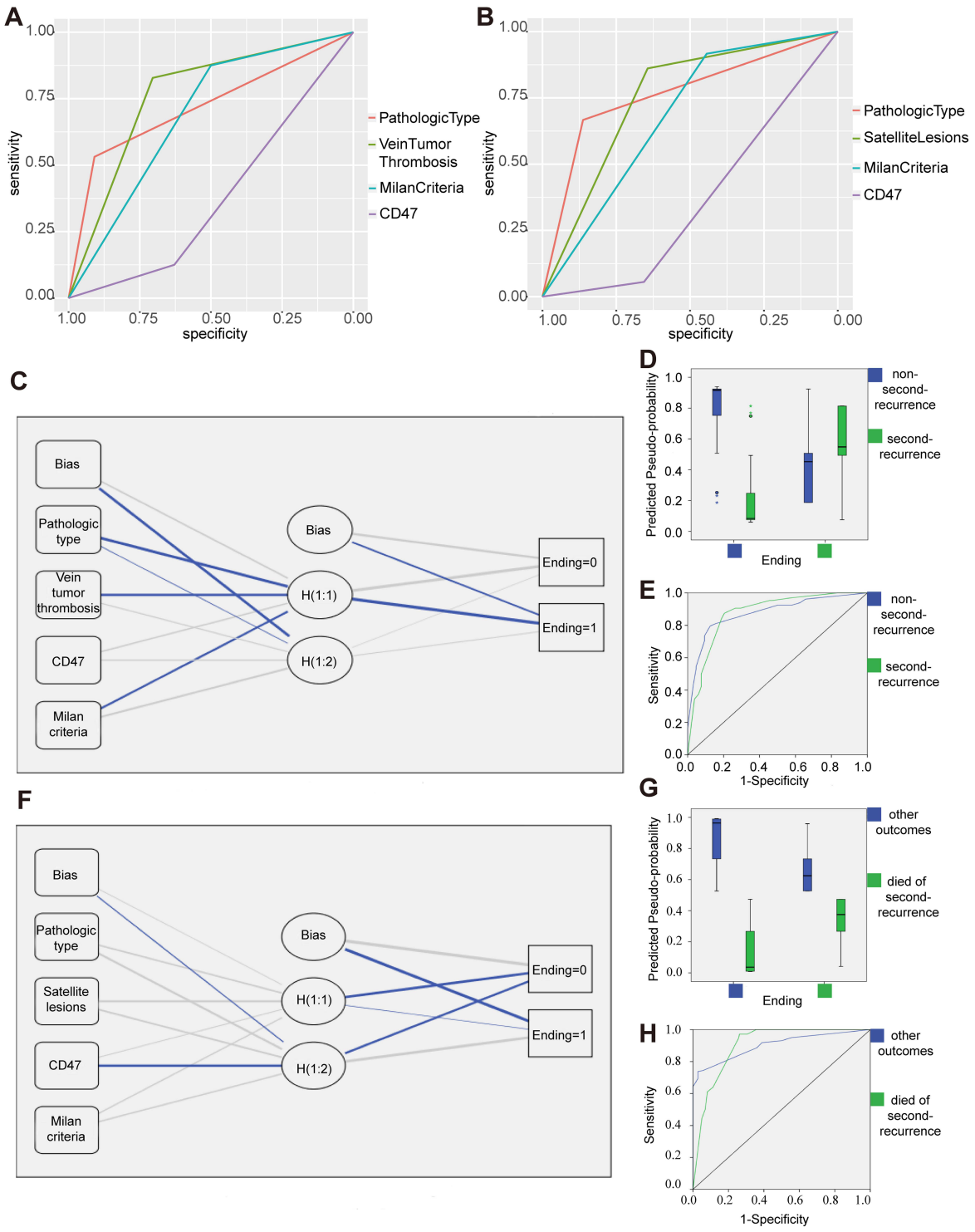

Figure 3 Architecture and performance of the ANN and the predictive capability via independent factors. (**A**) ROC curves for independent factors. ROC curve of the risk score showing its capacity in differentiating prognosis between non-second-recurrence and second -recurrence. ROC curves for independent factors. (**B**) ROC curves for independent factors. ROC curve of the risk score showing its capacity in differentiating prognosis between other outcomes and death from recurrence. ROC curves for independent factors. (**C**) ANN architecture. The network consisted of three layers: input (boxes 1–5), hidden (circles 1–3) and output (ending 0: nonrecurrence, ending 1: recurrence) layers. (**D**) ANN predicted-by-observed performance chart for non-second-recurrence and second-recurrence. (**E**) ANN predicted-by-observed separate ROC curves for non-second-recurrence and second-recurrence. (**F**) The network consisted of three layers: input (boxes 1–5), hidden (circles 1–3) and output (ending 0: other outcomes, ending 1: died of second recurrence) layers. (**G**) ANN predicted-by-observed performance chart for other outcomes and dying of second recurrence. ANN predicted-by-observed separate ROC curves for other outcomes and dying of second recurrence. (**H**) ANN predicted-by-observed separate ROC curves for other outcomes and dying of second recurrence.

https://doi.org/10.2147/CMAR.S566522

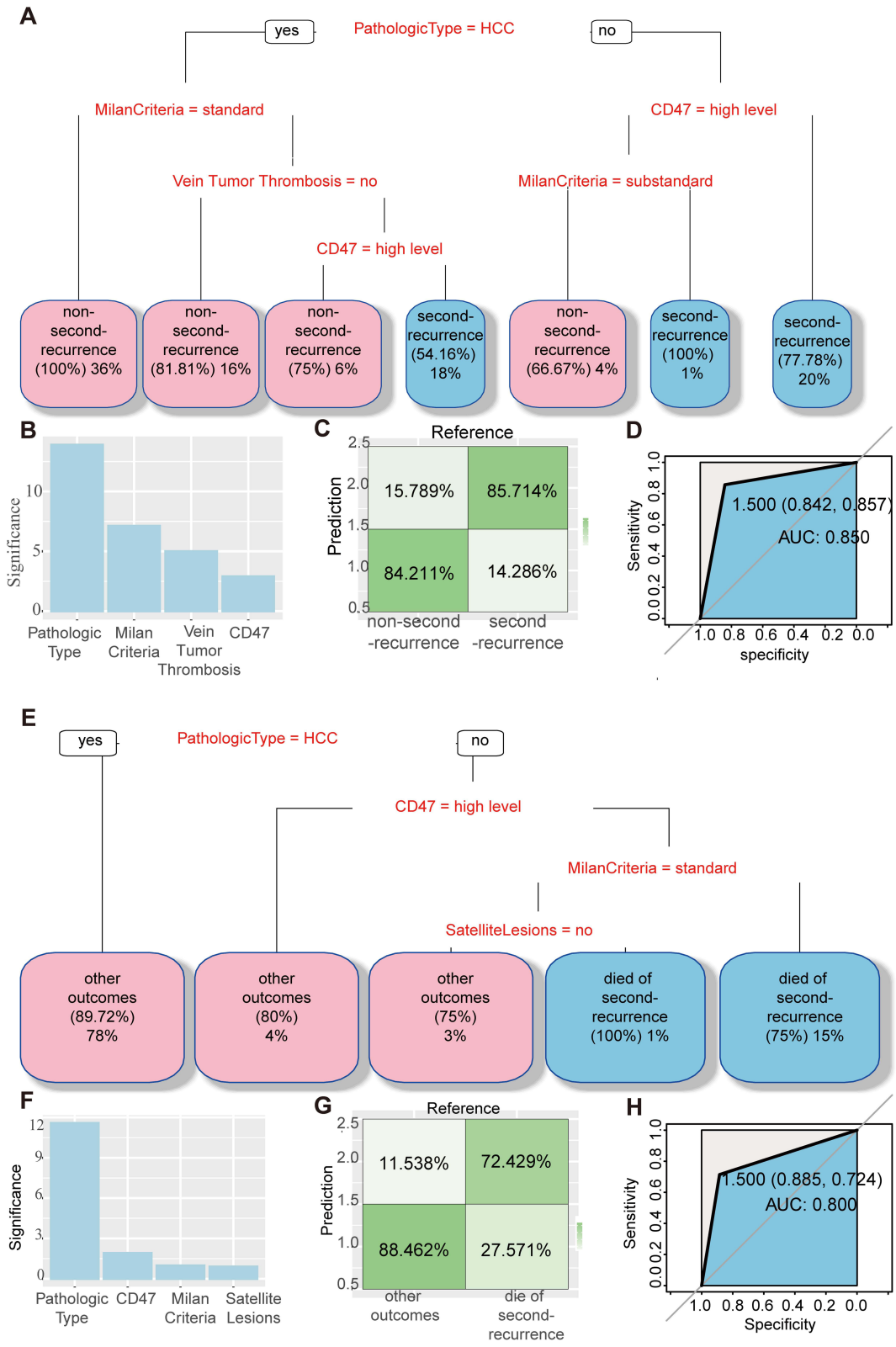

Figure 4 Classification tree and validation. (**A**) Classification tree of pathologic types, vein tumor thrombosis, Milan criteria, and CD47 for predicting non-second recurrence and second recurrence. (**B**) Significances of all factors by rank in the corresponding CART model. (**C**) CART model confusion matrix diagram reflecting the classification results in the corresponding CART model. (**D**) ROC curves of the corresponding CART model. (**E**) Classification tree of pathologic types, satellite lesions, and CD47 for predicting other outcomes and death of second recurrence. (**F**) Significance of all factors by rank in the corresponding CART model. (**G**) CART model confusion matrix diagram reflecting the classification results in the corresponding CART model. (**H**) ROC curves of the corresponding CART model.

https://doi.org/10.2147/CMAR.S566522

important variable (Figure 4F). However, this model showed lower performance in classifying patients who died from recurrence (72.43%, Figure 4G). The ROC curve (Figure 4H) indicated a sensitivity of 72.4%, specificity of 88.5%, and an AUC of 80.0%. K-fold cross-validation yielded a mean accuracy of 85.0%.

Notably, these models highlight the value of CD47 in prognostic prediction, particularly among patients with non-hepatocellular carcinoma pathologic types. Meanwhile, pathologic type consistently served as a strong clinicopathological predictor across both models.

Discussion

This study established predictive models for the postoperative second recurrence of hepatoma using clinicopathological factors and the immune-related biomarker CD47. The CART model integrates these variables to assist in managing recurrent hepatoma patients prior to secondary surgery. Given the high recurrence rate after surgical treatment,[18] this approach may help address a key clinical challenge by providing a practical and data-driven prognostic tool.

Our results suggest that CD47 serves as a useful diagnostic and prognostic biomarker. Among the clinicopathological factors analyzed, pathologic type, vein tumor thrombosis, Milan criteria, and satellite lesions were significant predictors of recurrence and survival. These findings align with previous reports showing that hepatocellular carcinoma (HCC) generally has a better prognosis,[19,20] while the Milan criteria, despite being considered restrictive, remain valuable in assessing recurrence risk.[21] Satellite lesions and vein tumor thrombosis are well-known indicators of tumor aggressiveness and poor outcomes in hepatoma patients.[22–25] Together, these adverse factors combined with CD47 expression enhance prognostic accuracy and may help identify patients at higher risk of second recurrence or disease-specific death.

The mean accuracy of the K-fold cross-validation of both models was 80.0% and 85.0%, respectively, which were very close to the corresponding AUC values, suggesting that our CART models are reliable.

ROC analysis demonstrated that combining these variables improved predictive accuracy compared with individual factors. Both the ANN and CART models achieved high accuracy (80–85%) and closely matched AUC values, confirming the reliability of the models. While the ANN model effectively captures complex, nonlinear relationships among variables,[26] the CART model provides a simpler, clinically interpretable structure that can be more readily applied by physicians.[27–30] The most clinically useful information gained by the CART models is that pathologic types are a priority factor in the prediction of postoperative recurrence and prognosis, followed by Milan criteria and CD47 in clinical application. CD47 can distinguish postoperatively second recurrence and prognosis for patients with non-HCC type hepatoma.

Interestingly, our findings on CD47 expression differ from several previous studies.[12,16,31] We observed that low CD47 expression was associated with poorer disease-specific survival and unfavorable pathological features, including advanced TNM stage, venous tumor thrombus, microvascular invasion (MVI), capsular invasion, and larger tumor size. This contrasts with the majority of studies suggesting that high CD47 expression promotes tumor proliferation, progression, and metastasis. Similar paradoxical observations have been reported in other cancers. For example, in non-small cell lung cancer, pancreatic neuroendocrine tumors, and certain hematologic or melanocytic malignancies, low or altered CD47 expression has not consistently correlated with poor prognosis.[32–36] Moreover, CD47 overexpression is absent in fibrolamellar hepatocellular carcinoma, a distinct subtype of hepatoma.[37] These findings suggest that the prognostic implications of CD47 may vary by tumor type and microenvironmental context.

As a single-center study, we uniquely focus on patients who have already experienced a first recurrence, representing a more advanced and biologically selected disease stage compared to the treatment-naïve cohorts typically examined in most studies. The role of immune checkpoints like CD47 may evolve with disease progression and prior therapeutic exposures, potentially explaining the discrepancy with literature derived from earlier-stage disease. Secondly, regarding the impact on clinical interpretation, our data suggest that the key value of CD47 in this setting is not as a generic marker of tumor aggression, but as a powerful independent prognostic marker specifically for predicting second recurrence and survival in this high-risk population. Its clinical utility lies in providing incremental predictive power beyond conventional clinical factors, potentially identifying a subgroup of patients with a distinct biological driver of recurrence. Moreover, an article investigating the clinicopathological and prognostic significance of CD47 expression in lung neuroendocrine tumors also found that,[38] contrary to its role in most hematologic and solid tumors, high CD47

expression in LNET patients was associated with better progression-free survival. The authors suggested that increased CD47 expression may promote the TSP-1–CD47 signaling pathway, thereby inhibiting angiogenesis, inducing tumor cell apoptosis, and modulating immune responses to enhance macrophage recruitment.[39] They further proposed that endocrine disturbances, such as those occurring in LNET and other hormone-secreting neuroendocrine cells, may exert a specific influence on the function of CD47. Although the liver is not primarily a hormone-secreting organ, it serves as a major target and metabolic site for multiple hormones and could therefore also be subject to certain regulatory effects.

This study has several limitations. First, only 36 patients (18.37%) died from second recurrence, which limits the statistical power and generalizability of the findings. Larger, multi-center cohorts are needed to further validate and refine these predictive models. Second, as this is a single-center, retrospective study, potential selection bias cannot be excluded. We plan to expand future research to include multi-institutional and prospective validation to enhance the robustness of our models.

In conclusion, we developed multi-factor prediction models integrating clinicopathological parameters and CD47 expression to forecast postoperative second recurrence and prognosis in hepatoma patients. These models may assist clinicians in postoperative management and preoperative planning for secondary surgery or transplantation.

Ethics Declarations

The sample collection was approved by the Clinical Research Ethic Committee of the First Affiliated Hospital, Zhejiang University School of medicine (approval number,2022-scientific research[1094]) and written informed consent was obtained from all participants.

Acknowledgments

We thank the patients and healthy volunteers who made this study possible and provided their samples.

Author Contributions

All authors made a significant contribution to the work reported, whether that is in the conception, study design, execution, acquisition of data, analysis and interpretation, or in all these areas; took part in drafting, revising or critically reviewing the article; gave final approval of the version to be published; have agreed on the journal to which the article has been submitted; and agree to be accountable for all aspects of the work.

Funding

This research did not receive any specific grant from funding agencies in the public, commercial, or not-for-profit sectors.

Disclosure

The authors have no conflicts of interest to declare.

References

1. Bray F, Ferlay J, Soerjomataram I, Siegel RL, Torre LA, Jemal A. Global cancer statistics 2018: GLOBOCAN estimates of incidence and mortality worldwide for 36 cancers in 185 countries. *CA Cancer J Clin*. 2018;68(6):394–424. doi:10.3322/caac.21492
2. Galle PR, Forner A, Llovet JM, et al. EASL clinical practice guidelines: management of hepatocellular carcinoma. *J Hepatol*. 2018;69(1):182–236. doi:10.1016/j.jhep.2018.03.019
3. de'Angelis N. Managements of recurrent hepatocellular carcinoma after liver transplantation: a systematic review. *World J Gastroenterol*. 2015;21(39):11185–11198. doi:10.3748/wjg.v21.i39.11185
4. Pommergaard H-C, Burcharth J, Rosenberg J, Rasmussen A. Serologic and molecular biomarkers for recurrence of hepatocellular carcinoma after liver transplantation: a systematic review and meta-analysis. *Transplantation Rev*. 2016;30(3):171–177. doi:10.1016/j.trre.2016.03.001.
5. Li X, Ramadori P, Pfister D, Seehawer M, Zender L, Heikenwalder M. The immunological and metabolic landscape in primary and metastatic liver cancer. *Nat Rev Cancer*. 2021;21(9):541–557. doi:10.1038/s41568-021-00383-9.
6. Holt DS, Botto M, Bygrave AE, Hanna SM, Walport MJ, Morgan BP. Targeted deletion of the CD59 gene causes spontaneous intravascular hemolysis and hemoglobinuria. *Blood*. 2001;98(2):442–449. doi:10.1182/blood.v98.2.442.
7. Hadders MA, Bubeck D, Roversi P, et al. Assembly and regulation of the membrane attack complex based on structures of C5b6 and sC5b9. *Cell Rep*. 2012;1(3):200–207. doi:10.1016/j.celrep.2012.02.003
8. Halme J, Sachse M, Vogel H, Giese T, Klar E, Kirschfink M. Primary human hepatocytes are protected against complement by multiple regulators. *Mol Immunol*. 2009;46(11–12):2284–2289. doi:10.1016/j.molimm.2009.04.005.

9. Fishelson Z. Obstacles to cancer immunotherapy: expression of membrane complement regulatory proteins (mCRPs) in tumors. *Mol Immunol*. 2003;40(2–4):109–123. doi:10.1016/s0161-5890(03)00112-3
10. Liu F, Luo L, Liu Z, et al. A genetic variant in the promoter of CD46 is associated with the risk and prognosis of hepatocellular carcinoma. *Molecular Carcinogenesis*. 2020;59(11):1243–1255. doi:10.1002/mc.23252
11. Lu Z, Zhang C, Cui J, et al. Bioinformatic analysis of the membrane cofactor protein CD46 and microRNA expression in hepatocellular carcinoma. *Oncol Rep*. 2014;31(2):557–564. doi:10.3892/or.2013.2877
12. Lo J, Lau EYT, So FTY, et al. Anti- CD 47 antibody suppresses tumour growth and augments the effect of chemotherapy treatment in hepatocellular carcinoma. *Liver Int*. 2016;36(5):737–745. doi:10.1111/liv.12963
13. Xiao Z, Chung H, Banan B, et al. Antibody mediated therapy targeting CD47 inhibits tumor progression of hepatocellular carcinoma. *Cancer Lett*. 2015;360(2):302–309. doi:10.1016/j.canlet.2015.02.036
14. Jaiswal S, Jamieson CHM, Pang WW, et al. CD47 is upregulated on circulating hematopoietic stem cells and leukemia cells to avoid phagocytosis. *Cell*. 2009;138(2):271–285. doi:10.1016/j.cell.2009.05.046
15. Willingham SB, Volkmer J-P, Gentles AJ, et al. The CD47-signal regulatory protein alpha (SIRPa) interaction is a therapeutic target for human solid tumors. *Proc Natl Acad Sci USA*. 2012;109(17):6662–6667. doi:10.1073/pnas.1121623109
16. Chen J, Zheng D-X, Yu X-J, et al. Macrophages induce CD47 upregulation via IL-6 and correlate with poor survival in hepatocellular carcinoma patients. *Oncoimmunology*. 2019;8(11):e1652540. doi:10.1080/2162402x.2019.1652540
17. Sun Y, Wu L, Zhong Y, et al. Single-cell landscape of the ecosystem in early-relapse hepatocellular carcinoma. *Cell*. 2021;184(2):404–21.e16. doi:10.1016/j.cell.2020.11.041
18. Yamashiki N, Yoshida H, Tateishi R, et al. Recurrent hepatocellular carcinoma has an increased risk of subsequent recurrence after curative treatment. *J Gastroenterol Hepatol*. 2007;22(12):2155–2160. doi:10.1111/j.1440-1746.2006.04732.x
19. Hu JY, Zhou HB, Liu WD, Zhang J, Hu HP, Liu J. A comparative study of intrahepatic cholangiocarcinoma and hepatocellular carcinoma with reference to clinical features and prognosis. *Zhonghua Gan Zang Bing Za Zhi*. 2019;27(7):511–515. doi:10.3760/cma.j.issn.1007-3418.2019.07.007.
20. Wang X, Wang W, Ma X, et al. Combined hepatocellular-cholangiocarcinoma: which preoperative clinical data and conventional MRI characteristics have value for the prediction of microvascular invasion and clinical significance? *Eur Radiol*. 2020;30(10):5337–5347. doi:10.1007/s00330-020-06861-2
21. Gunsar F. Liver transplantation for hepatocellular carcinoma beyond the milan criteria. *Experim Clinl Transplant*. 2017;15(Suppl 2):59–64. doi:10.6002/ect.TOND16.L16.
22. Shen J, Wen T, Chen W, Lu C, Yan L, Yang J. Model predicting the microvascular invasion and satellite lesions of hepatocellular carcinoma after hepatectomy. *ANZ J Surg*. 2018;88(11):E761–e66. doi:10.1111/ans.14473.
23. Yang JD, Kim RW, Park KW, et al. Model to estimate survival in ambulatory patients with hepatocellular carcinoma. *Hepatology*. 2012;56(2):614–621. doi:10.1002/hep.25680
24. Yang Z, Luo F-Z, Wang S, et al. Alpha-fetoprotein and 18F-FDG standard uptake value predict tumor recurrence after liver transplantation for hepatocellular carcinoma with portal vein tumor thrombosis: preliminary experience. *Hepatobiliary Pancreatic Dis Int*. 2020;19(3):229–234. doi:10.1016/j.hbpd.2020.03.009
25. Khan AR, Wei X, Xu X. Portal vein tumor thrombosis and hepatocellular carcinoma – the changing tides. *J Hepatocellular Carcinoma*. 2021;8:1089–1115. doi:10.2147/jhc.S318070
26. Zhang Z, Beck MW, Winkler DA, Huang B, Sibanda W, Goyal H. Opening the black box of neural networks: methods for interpreting neural network models in clinical applications. *Ann translat Med*. 2018;6(11):216. doi:10.21037/atm.2018.05.32.
27. Hong W, Dong L, Huang Q, Wu W, Wu J, Wang Y. Prediction of severe acute pancreatitis using classification and regression tree analysis. *Dig Dis Sci*. 2011;56(12):3664–3671. doi:10.1007/s10620-011-1849-x.
28. Wu BU, Johannes RS, Sun X, Tabak Y, Conwell DL, Banks PA. The early prediction of mortality in acute pancreatitis: a large population-based study. *Gut*. 2008;57(12):1698–1703. doi:10.1136/gut.2008.152702.
29. Augustin S, Muntaner L, Altamirano JT, et al. Predicting early mortality after acute variceal hemorrhage based on classification and regression tree analysis. *Clin Gastroenterol Hepatol*. 2009;7(12):1347–1354. doi:10.1016/j.cgh.2009.08.011
30. Hong W-D, Dong L-M, Jiang Z-C, Zhu Q-H, Jin S-Q. Prediction of large esophageal varices in cirrhotic patients using classification and regression tree analysis. *Clinics*. 2011;66(1):119–124. doi:10.1590/s1807-59322011000100021.
31. Kim H, Bang S, Jee S, Paik SS, Jang K. Clinicopathological significance of CD47 expression in hepatocellular carcinoma. *J Clin Pathol*. 2021;74(2):111–115. doi:10.1136/jclinpath-2020-206611.
32. Arrieta O, Aviles-Salas A, Orozco-Morales M, et al. Association between CD47 expression, clinical characteristics and prognosis in patients with advanced non-small cell lung cancer. *Cancer Med*. 2020;9(7):2390–2402. doi:10.1002/cam4.2882
33. Imam R, Chang Q, Black M, Yu C, Cao W. CD47 expression and CD163+ macrophages correlated with prognosis of pancreatic neuroendocrine tumor. *BMC Cancer*. 2021;21(1):320. doi:10.1186/s12885-021-08045-7.
34. Yanagida E, Miyoshi H, Takeuchi M, et al. Clinicopathological analysis of immunohistochemical expression of CD47 and SIRPα in adult T-cell leukemia/lymphoma. *Hematologic Oncol*. 2020;38(5):680–688. doi:10.1002/hon.2768
35. Nath PR, Pal-Nath D, Mandal A, Cam MC, Schwartz AL, Roberts DD. Natural killer cell recruitment and activation are regulated by CD47 expression in the tumor microenvironment. *Cancer Immunol Res*. 2019;7(9):1547–1561. doi:10.1158/2326-6066.Cir-18-0367.
36. Galli S, Zlobec I, Schürch C, Perren A, Ochsenbein AF, Banz Y. CD47 protein expression in acute myeloid leukemia: a tissue microarray-based analysis. *Leukemia Res*. 2015;39(7):749–756. doi:10.1016/j.leukres.2015.04.007.
37. Cooney T, Wei MC, Rangaswami A, Xu L, Sage J, Hazard FK. CD47 is not over-expressed in fibrolamellar hepatocellular carcinoma. *Ann Clin Lab Sci*. 2017;47(4):395–402.
38. Orozco-Morales M, Avilés-Salas A, Hernández-Pedro N, et al. Clinicopathological and prognostic significance of CD47 expression in lung neuroendocrine tumors. *J Immunol Res*. 2021;2021:6632249. doi:10.1155/2021/6632249
39. Gao L, Chen K, Gao Q, Wang X, Sun J, Yang Y-G. CD47 deficiency in tumor stroma promotes tumor progression by enhancing angiogenesis. *Oncotarget*. 2017;8(14):22406–22413. doi:10.18632/oncotarget.9899